Chapter

Neurotoxin Decontamination

Dongmei Ye and Susan Rempe

Abstract

Nerve agents are a group of organophosphorus (OP) compounds that are potent neurotoxins used as chemical warfare agents and insecticides. Current medical countermeasures, including atropine and oxime-based reactivators, target the down-stream pathways inhibited by OP agents and cannot effectively eliminate OP agents. In contrast, organophosphorus hydrolase (OPH) is a bacterial enzyme that can detoxify a wide range of OP agents. The advantage of OPH over oxime-based treatment is rapid hydrolysis of these agents in the circulatory system. Kinetic properties of OPH from various bacteria have been studied by others. Substrate binding affinity ranges between 200 μM and 2.5 mM, well above lethal levels. To improve OPH mutant screening capability, we optimized a cell-free protein synthesis system to express active OPH variants rapidly and conduct kinetic measurements. We also tested the hypothesis that active site mutations using only natural amino acids restrict the development of OPH variants with binding affinities close to nerve agent lethal levels (a few μM). Our work resulted in a suite of OPH variants that incorporated selected unnatural amino acids into OPH, with mutations targeted for the first time to both active and allosteric binding sites. Kinetic studies of those mutants show significantly improved OPH substrate binding affinity.

Keywords: organophosphorus hydrolase, nerve agent, paraoxon, substrate binding affinity, unnatural amino acid substitution

1. Introduction

As a neurotransmitter, acetylcholine (ACh) plays a vital role in brain and muscle function. Its function can be both excitatory and inhibitory. But in the central nervous system (CNS), ACh primarily plays the excitatory role, which means it can speed up nerve signals. Excess ACh is degraded by acetylcholinesterase (AChE) to maintain a balanced ACh level. Nerve agents are a group of organophosphorus (OP) compounds that are potent neurotoxins used as chemical warfare agents and insecticides. OP nerve agents disrupt the CNS by inhibiting AChE function. Inhibition of AChE results in ACh accumulation and ACh receptor overstimulation, leading to severe injuries and even death due to losing control of respiratory muscles. Those injured by nerve agents often express chronic health problems, such as visual impairment, dermatological conditions, neurological sequelae, and respiratory problems [1].

Weapons of mass destruction were first used in World War I. Rapid advances in chemistry during that time brought surging knowledge and constant growth in developing more effective chemical agents. The nerve agent, tabun, was first discovered

from an organophosphorus insecticide in 1936 by a German chemist, Dr. Gerhart Schrader. About two years later, Dr. Schrader developed another similar nerve agent, sarin [2]. Suitable delivery systems and large-scale production of nerve agents were also developed rapidly for their usage in warfare. Since nerve agents are stable, easily dispersed and work at low concentrations, the effects are long-lasting and increase with continued exposure. The threat from nerve agents was not confined to military battlefields. The Matsumoto sarin attack (1994) and Tokyo subway sarin attack (1995) exhibited the usage of nerve agents in terrorist attacks. Paraoxon, which is the active metabolite of the insecticide parathion, is also a potent nerve agent. As such, nerve agents pose a threat to armed forces, agricultural workers, and civilians.

Current medical countermeasures available include atropine and pralidoxime chloride (2-PAM Cl). Atropine competitively inhibits ACh binding to acetylcholine receptors, reducing receptor overstimulation. The therapeutic 2-PAM Cl re-cleaves AChE phosphorylation induced by nerve agents and reactivates AChE. These countermeasures target the down-stream pathways of OP; thus, none of them effectively eliminates OP agents.

A direct method that can hydrolyze OP agents before they enter the central nervous system is urgently needed. Organophosphorus hydrolase (OPH) is a bacterial enzyme that can detoxify a wide range of OP nerve agents and pesticides. The advantage of OPH over existing treatments is rapid hydrolysis of OP agents, which provides the potential to eliminate nerve agents in the circulatory system, before they penetrate the blood-brain barrier and exert effects in the CNS. Kinetic properties of OPH from various bacteria have been studied, with k_{cat} about 10^3/s–10^4/s and K_m between 80 μM and 2.5 mM [3, 4], significantly higher compared to nerve agent lethal levels (a few μM).

The OPH active site is dominated by histidine residues and stabilized by the stacking network formed among these histidine residues. This unique feature makes OPH a great candidate for aromatic unnatural amino acid (UAA) substitutions.
In this chapter, we first describe a high-throughput cell-free protein synthesis and kinetic measurement method for rapid screening and selection of OPH variants with enhanced substrate binding. Then, we examine the possibility to apply cell-free protein synthesis systems for expression of OPH UAA substitutions. Lastly, we present a genetic code expansion (GCE) machinery used to examine the expression of OPH UAA substitutions. The results of kinetic studies of these mutants showed greatly improved OPH substrate binding affinity. Overall, this work uniquely demonstrates that UAA replacements can enhance enzyme properties significantly.

2. Bio-engineered OPH degradation of nerve agent analog: paraoxon

2.1 Methods

2.1.1 Identify OPH mutation sites with molecular simulation

Computational studies, to identify OPH mutation sites, used chain A of the OPH crystal structure of paraoxon analog and diethyl 4-methylbenzylphosphonate, co-crystallized with OPH [5]. In contrast to most previous structural studies, which assumed that the binding orientation of paraoxon resembles the substrate analog [6–8], we identified a different binding mode for paraoxon compared to its analog diethyl 4-methylbenzylphosphonate [9]. To do this, we used three different docking algorithms (POSIT, HYBRID, and FRED) available in OPENEYE software

(OEDocking 3.2.0, OpenEye Inc.) to generate fifty potential binding modes of paraoxon in the OPH binding site. After down-selecting to the two most dissimilar paraoxon-OPH docking poses, we carried out molecular dynamics (MD) simulations over long times, up to 105 ns, to obtain the most stable paraoxon binding mode and define binding interactions at the OPH active site. MD simulation was also performed to identify mutation sites that can stabilize paraoxon binding.

Details of the MD simulations can be found in Ref. [9]. In brief, we used the OpenMM simulation package 7.11. We assigned partial charges to the substrate (paraoxon) atoms using the AM1-BCC charge model [10]. Amberff14SB and GAFF vs. 1.8 force fields were applied to the protein and substrate, respectively. We applied the TIP3P force field to describe water. After solvating the protein-substrate complex in water in a cubic box of 10 Å on a side, Na^+ and Cl^- counter ions were added to neutralize the system. We set the simulation time step to 4 fs and applied the hydrogen mass repartitioning approach [11, 12]. Long-ranged electrostatic interactions were calculated using the particle mesh Ewald approach [13], with a cut-off of 10 Å for the real-space electrostatic and Lennard-Jones forces. After minimizing the energy of the water and ions, while keeping the protein and substrate restrained using 500 kcal/mol-$Å^2$ positional restraints, we performed a second energy minimization step.

2.1.2 Cell-free protein synthesis of OPH variants

The rapid cell-free protein expression system can screen hundreds of variants per day in 200 μl reactions. The activity of the expressed product and substrate binding affinity also can be measured directly in the expression mixture, eliminating time-consuming and labor-intensive cell culture-based protein expression and purification processes. A wheat germ cell-free protein synthesis system from Cell-Free Science was used to generate wild type (WT) and mutant OPH. WT and mutant OPH plasmids were cloned into a pEU-E01 vector. The cell-free expression reaction is detailed here: 20 μl of transcription reactions containing 4 μl of 5x transcription buffer, 2 μl of NTP mix, 0.25 μl of RNase inhibitor, 0.25 μl of SP6 RNA polymerase, and 2 μl of plasmid are prepared and incubated at 37°C for 6 h, and then, translation reactions containing 10 μl of transcription reaction, 0.8 μl of creatine kinase (1 mg/ml), 10 μl of WEPRO, 75 μM of $Zn(OAc)_2$, and 206 μl of SUB-MIX are prepared and incubated at 15°C for 20 h. OPH variant expression in the cell-free reaction mixture was detected using SDS-gel. A series dilution of purified recombinant OPH was used as standards and loaded with cell-free generated OPH to a SDS gel, and OPH variant concentrations were determined by densitometry.

We also explored, for the first time, the possibility of using cell-free protein synthesis to express OPH with UAA substitutions. The small reaction volumes minimize the need for large quantities of UAAs. The plasmid encoding UAA tRNA/tRNA synthetase pair can be co-translated in the same cell-free reaction with expression protein; thus, the expensive and tricky re-engineering of living cellular expression systems is not required to accommodate a new genetic code for UAAs. In addition, the cell-free protein synthesis system's open access to transcription and translation simplifies protein expression optimization. To increase the chance of success, both wheat-germ and PURExpress cell-free system were used in this study. Six OPH mutants containing the amber codon for UAA substitution were constructed into both the PURExpress vector and pEU-E01 vector. Pilots of expression screening were performed with either co-translation of pAcFRS plasmid with OPH mutant plasmids in the same cell-free reaction or substitute reaction with pAcFRs protein and tRNA.

Ten UAAs were screened at various reaction conditions, including 4-acetyl-L-phenylalanine, 3,4 dihydroxy-L-phenylalanine, 1-methyl-L-histine, 4-amino-L-phenylalanine, 4,4,4,4,4,4-hexafluoro-valine, p-fluoro-phenylalanine, 5,5,5-trifluoro-leucine, 3,3,3-trifluoro-alanine, 1–4-thiazolylalanine, and L-3-thienylalanine. Only 4-acetyl-L-phenylalanine showed some level of expression in both cell-free systems, but kinetic measurement did not detect any activity on this UAA substitution. This expression was not confirmed beyond visual observation of a SDS gel band since this substitution was not active kinetically. More work can be done in the future by researchers who desire to advance the cell-free protein expression capability.

2.1.3 OPH UAA variant expression in cell culture

Eight OPH mutants containing an amber codon for UAA substitution were generated by GenScript. OPH-H55TAG, H57TAG, H201TAG, H230TAG, H254TAG, H257TAG, D253TAG, and D253E/H254TAG were cloned into pET24b(+) vector using NdeI/XhoI sites for expression in an *E. coli* host. The WT and mutant OPH cloned into pET24b(+) vector were co-transformed into the *E. coli* strain BL21 ai with proper GCE plasmids (**Table 1**). WT-GFP and GFP-150 plasmids were used as positive controls for UAA substitution. The cells were grown in standard LB supplemented with 1 mM UAA and induced by 0.2% L-arabinose and 1 mM IPTG at 16°C overnight. Cells were harvested by centrifugation at 4500 g for 15 min and resuspended in Ni-NTA lysis buffer: 50 mM NaH2PO4, 300 mM NaCl, 10 mM imidazole, and 0.1 μM pepstatin at a pH of 7.4. The cells were lysed using Microfluidizer (Microfluidics Corp, Westwood, MA) and then centrifuged at 12,000 g for 30 min. The collected supernatant was incubated with 5 ml of Ni-NTA resin under end-to-end shaking and loaded on a 5 mL HisTrap FF column. After washing with wash buffer containing 50 mM NaH_2PO_4, 300 mM NaCl, 20 mM imidazole, the proteins were eluted by elution

Mutant plasmid	Antibiotic resistance	GCE plasmid	Antibiotic resistance	UAA
H257TAG	Kanamycin (Kan)	pDulo-halo	Spectinomycin (Spec)	3,4-Dihydroxy-L-phenylalanine
H257TAG	Kan	pDulo-halo	Spec	3-BromoTyrosine
H257TAG	Kan	pDulo-pAminoPhe	Spec	4-Amino-L-phenylalanine
H55TAG	Kan	pEvol-pylRS-mjH	Chloramphenicol (Chl)	3-Methyl-Histine
H57TAG	Kan	pEvol-pylRS-mjH	Chl	3-Methyl-Histine
H201TAG	Kan	pEvol-pylRS-mjH	Chl	3-Methyl-Histine
H230TAG	Kan	pEvol-pylRS-mjH	Chl	3-Methyl-Histine
H254TAG	Kan	pEvol-pylRS-mjH	Chl	3-Methyl-Histine
H257TAG	Kan	pEvol-pylRS-mjH	Chl	3-Methyl-Histine
D253TAG	Kan	pEvol-pylRS-mjH	Chl	3-Methyl-Histine
D253E/H254TAG	Kan	pEvol-pylRS-mjH	Chl	3-Methyl-Histine

Table 1.
GCE plasmid and UAA combination used for co-transformation.

buffer containing 50 mM NaH_2PO_4, 300 mM NaCl, 250 mM imidazole. Elution fractions containing OPH UAA variants were pooled together and concentrated using a protein concentrator from Thermo Scientific.

2.1.4 Spectrophotometric assay of OPH variant activity

For cell-free synthesized OPH variants, their activities and substrate binding affinities were measured directly in the cell-free reaction mixture using a BioTek plate reader (Winooski, VT) and that reported light absorbance of the paraoxon leaving group at 405 nm. The assay conditions for cell-free expression were carried out by adding various amounts of paraoxon (final concentration: 0.1, 0.2, 0.5, 1.0, 2.0 and 3.0 mM) to 193.7 μL of buffer containing 100 mM CHES and 75 μM of $Zn(OAc)_2$, at pH = 9.0. The reactions were started by adding 2 μL of cell-free generated WT or OPH variants.

The kinetic assays of OPH UAA variants were performed also by measuring the absorbance of the paraoxon leaving group at 405 nm, as mentioned above. The changes of absorbance at 405 nm over time were used to calculate initial catalytic velocities as a function of the various substrate concentrations. Then, the initial velocity data, along with corresponding paraoxon concentrations, were plotted and analyzed by the Michaelis-Menten equation to obtain V_{max} and K_m using GraphPad (GraphPad Software, Inc., La Jolla, CA, USA). The k_{cat} was calculated by the ratio of V_{max} and mutant concentration. Each kinetic measurement condition was performed in triplicate and standard deviation was calculated using GraphPad.

2.2 Results

2.2.1 Identify OPH UAA mutation sites with increased active site stability

OPH used in this study is a homodimer from *Pseudomonas diminuta*. The OPH crystal structure 1HZY [1] contains 330 amino acids and two Zn(II) metal cations in Chain A. One Zn(II) coordinates with active site residues H201, H230 and two water molecules. The other Zn(II) coordinates with active site residues H55, H57, D301 and one water molecule [9]. Though OPH's natural substrate and function remains unknown, it is very effective at hydrolyzing the P—O bond of the phosphotriester insecticide paraoxon. OPH can also hydrolyze a wide spectrum of OP compounds containing phosphotriester (P—O), phosphonothioate (P—S), phosphonofluoridate (P—F), and phosphonocyanate (P—CN) bonds [14, 15].

Many previous studies on OPH focused only on altering the active site residues to achieve catalytic efficiency and substrate specificity. In this chapter, we extended our study of the OPH active site to include nearby active site residues as well, using the novel allosteric regulation approach. We targeted the residues near OPH active sites that do not coordinate with metal cations and are not involved in the hydrolysis reaction, but can form H-bonds with active site residues. In that way, we identified D253, which forms an H-bond with H230. An interesting observation about OPH is that its active site is dominated by four histidine residues: H55, H57, H201, and H230 (**Figure 1**). H254 and H257 also form an aromatic stacking network at the active site, while H257 plays an important role in stabilizing OPH [16]. We found that histidine's aromatic structure made it a great candidate for aromatic UAA substitution. Alterations of these histidine residues with UAA were achieved for examination of a more stable substrate binding reaction.

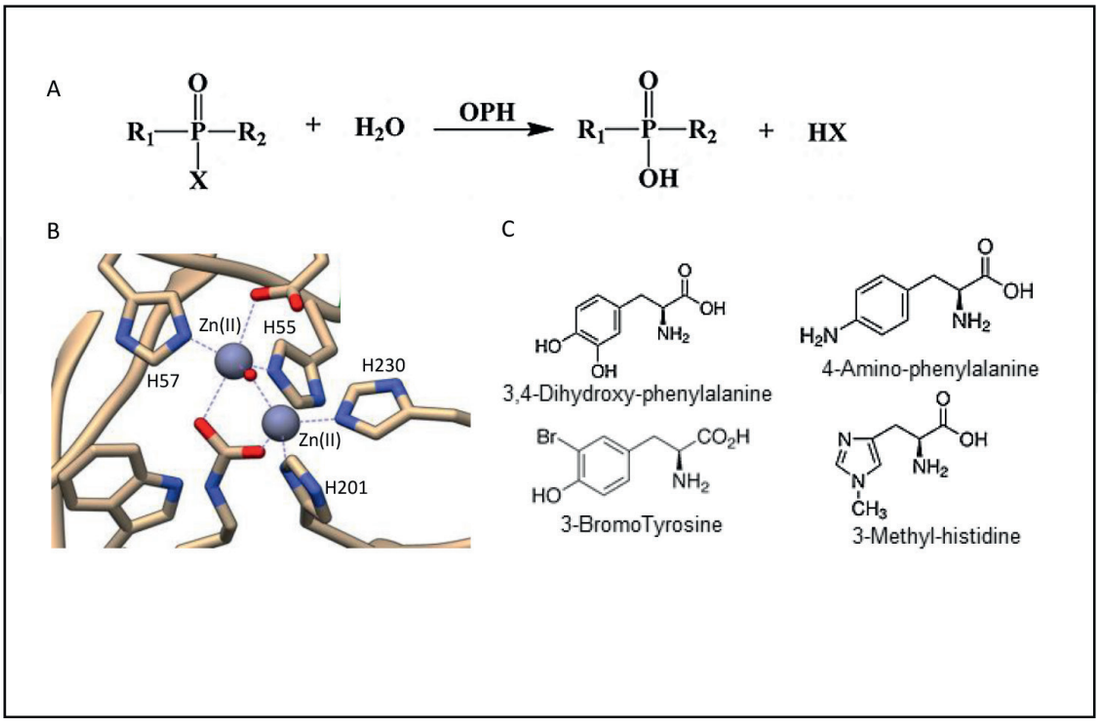

Figure 1.
A. Schematic diagram of OPH catalyzed hydrolysis reaction. B. OPH active site showing all four histidine residues and their interaction with Zn(II). C. Structure of UAAs used in this study.

2.2.2 Cell-free protein synthesis of OPH variants with increased thermal stability and substrate binding affinity

Despite the high-throughput advantage, a big challenge for many researchers has been how to maintain kinetic activity of expressed protein in cell-free protein synthesis system. Through screening of the cell-free reaction conditions, we have determined that the amount of creatine kinase played a key role in the success of OPH variant expression. Creatine kinase concentration was optimized and a large number of OPH variants were generated successfully using the cell-free protein synthesis system. Kinetic measurements were performed directly using the cell-free reaction mixture. Results of single mutation at D253E and double mutations at D253E/H254R both have improved paraoxon binding. Detailed study on OPH structure and kinetics on these two variants are reported in our recent publication [9]. In a separate study, we were interested in two threonine residues at allosteric location 54 and 199. We have examined the potential to replace threonine with a larger amino acid isoleucine to fill in the gap in OPH structure, therefore, to achieve active site stabilization. Single mutation at T199I and double mutation at T199I/T54I were not able to improve paraoxon binding affinity, but both mutations increased OPH kinetic activity up to 200-fold compared to WT OPH at temperature up to 60°C (manuscript under preparation), which shined light on OP agent remediation that requires OPH to function at elevated temperatures.

2.2.3 OPH UAA mutant expression in E. coli host

UAA substitution at H257 site was selected as an example to show expression level over time. The 4-amino-L-phenylalanine, 3,4-dihydroxy-L-phenylalanine, and

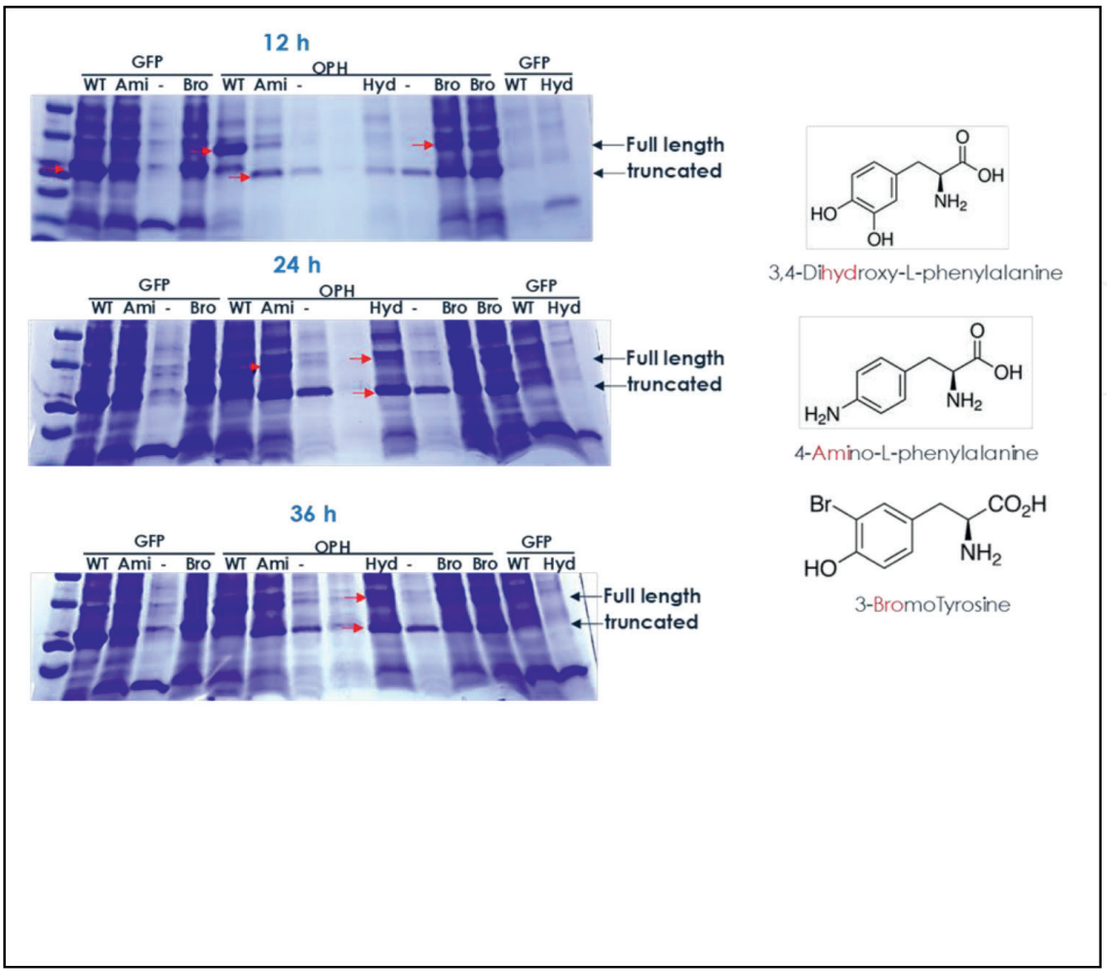

Figure 2.
Time course of OPH UAA substitution expression. Three UAAs were tested for expression over a time period of 36 h. GFP plasmids were used as positive control. UAA expression was detected starting at 12 h, and maintained up to 36 h. Letter abbreviations of UAA's full names are colored in red and to label UAA expression on SDS gels.

3-bromotyrosine substitutions at H257 were successfully expressed (**Figure 2**) over a 36-hour time period. Both 4-amino-L-phenylalanine and 3-bromotyrosine substitutions expressed at a relatively earlier time around 12 h, followed by 3,4-dihydroxy-L-phenylalanine substitution expression starting around 24 h. All substitutions are consistently expressed up to 36 h. The 3-methyl-histine substitution was also successfully expressed at H55, H57, H201, H230, H254, and H257. The 3-methyl-histine mutant expression level was higher than other three UAA substitutions due to close structural similarity to histidine.

2.2.4 Spectrophotometric assay of OPH UAA variant activity

The catalysis of P-O bond cleavage of paraoxon was monitored using a continuous spectrophotometric assay. Both k_{cat} and K_m values were measured and compared to WT OPH (**Table 2**). The 3,4-dihydroxy-L-phenylalanine substitution at H257 did not have any detectable activity. 4-amino-L-phenylalanine and 3-bromotyrosine substitutions at H257 resulted in a K_m of 0.018 mM and 0.073 mM, respectively (**Table 2**). The 4-amino-L-phenylalanine substitution at H257 improved paraoxon binding by 4.6-fold compared to WT OPH, while 3-bromo-tyrosine substitution at H257 did not improve paraoxon binding compared to WT OPH. Catalytic rates, k_{cat}, for these

	k_{cat} (s^{-1})	K_m (mM)	K_m fold improvement
WT OPH	25750.0 ± 2060.6	0.0835 ± 0.0186	—
H257-AminoPhe	—	0.0180 ± 0.0062	4.6
H257-BromoTyr	—	0.0728 ± 0.0146	1.1
H257-HydroxyPhe	—	—	—
H55-MethylHis	588.9 ± 27.3	0.0265 ± 0.0055	3.2
H57-MethylHis	221.0 ± 24.2	0.2346 ± 0.0719	0.36
H201-MethylHis	2.5 ± 0.1	0.0174 ± 0.0024	4.8
H230-MethylHis	4.9 ± 0.1	0.0058 ± 0.0005	14.4
H254-MethylHis	25.6 ± 0.9	0.0254 ± 0.0046	3.3
H257-MethylHis	56.0 ± 3.0	0.0459 ± 0.0096	1.8
D253-MethylHis	2.0 ± 0.2	0.2137 ± 0.0660	0.4
D253E-H254MethylHis	2.6 ± 0.3	0.0991 ± 0.0318	0.8

Table 2.
The k_{cat} and K_m measured for WT and mutant OPH.

mutants were not calculated due to low protein concentration after elution from Ni-NTA column, which made protein concentration measurement impossible.

Non-histidine residue UAA substitution at D253 was not able to improve substrate binding. This aligns with our hypothesis that our selected UAAs are more suitable for histidine replacement.

All 3-methyl-histine substitutions are kinetically active (**Table 2**). The 3-methyl-histine substitution at H230 resulted in the most improvement among all mutants, with a 14.4-fold increase in paraoxon binding. The 3-methyl-histine substitution at H55 was the most active mutant, with a 3.2-fold increase in paraoxon binding.

2.3 Discussion

An effective enzyme bio-engineering approach starts by the identification of key amino acid residues that, when altered, improve the activity of the targeted enzyme. Many successes have been demonstrated through the development of small molecule binding proteins [17] and redesign of enzyme binding sites to either accommodate a new substrate [18] or engineer novel catalytic sites [19, 20]. A few promising results in developing potential therapeutics have examined the applications of allosteric regulations in protein engineering [21–30].

OPH is capable of hydrolyzing a wide spectrum of OP compounds, but its application in neurotoxin degradation was limited due to insufficient substrate binding affinity. In our previous project on developing thermally stable OPH variants, we utilized an allosteric network modulation algorithm and molecular design suite "Eris" [31, 32]. Hotspots that enhanced allosteric network stability were identified and we produced dozens of OPH mutants exhibiting enhanced kinetics for paraoxon, but none of them improved substrate binding. Saturation mutagenesis done by Chen et al. also failed to tighten substrate binding [33].

In this work, we investigated the potential of using UAA substitutions to improve OPH substrate binding. OPH has a unique active site structure packed with histidine residues. These histidine residues form aromatic stacking network and H-bond with

substrate. Three GCE plasmids and four UAAs were tested successfully for OPH UAA expression. Among four UAA substitutions, 3,4-dihydroxy-L-phenylalanine substitution not only needed longer time to express, but also resulted in no detectable activity. The 3-bromotyrosine substitutions expressed well, with low yield after purification, but this substitution was not able to improve substrate binding. These observations eliminate both compounds from the potential UAA substitution list. The 4-amino-L-phenylalanine substitution expressed well, with a low protein yield after purification. This result makes kinetic measurement difficult. With a 4.6-fold improvement on substrate binding, further optimization on protein expression could still make 4-amino-L-phenylalanine a good UAA substitution candidate. The 3-methyl-His replacement achieved the highest protein expression level, and the 3-methyl-His replacement at H230 expressed the highest improvement on paraoxon binding. 3-methyl-His replacement at H230 was able to bring K_m down to 5.8 μM, close to the nerve agent lethal dose. Since H230 is located at the OPH active site, the 3-methyl-His replacement also reduced the turnover rate of this mutation. Force fields for these UAAs are not currently available, so MD simulation cannot yet be used to examine UAA orientations at the active site nor any formation of H-bond after UAA substitution. The goal of this study is to demonstrate the proof-of-concept of the feasibility of using UAA substitution to stabilize the OPH active site and improve substrate binding affinity. Our results are promising and provide new insight into OPH bioengineering.

2.4 Conclusion

In this chapter, we demonstrated the high-throughput of cell-free protein synthesis in enzyme kinetic studies. We also explored the possibility of using UAA to enhance OPH substrate binding by testing a method utilizing GCE machinery to incorporate selected UAAs into OPH. A TAG stop codon was inserted into OPH to replace these sites, and OPH mutants with UAA substitution were expressed successfully. A total of eleven UAA substitutions were generated, with 3-methyl-histine substitutions identified as the most suitable to replace the OPH active site histidine network. Results of kinetic studies of these mutants show significantly improved OPH substrate binding affinity.

Acknowledgements

The team would like to thank Sandia's LDRD program.

Sandia National Laboratories (SNL) is a multi-mission laboratory managed and operated by National Technology & Engineering Solutions of Sandia, LLC, a wholly owned subsidiary of Honeywell International Inc., for the U.S. Department of Energy's National Nuclear Security Administration under contract DE-NA0003525. This work was supported by Sandia's LDRD program. The views expressed in the article do not necessarily represent the views of the U.S. Department of Energy or the United States Government.

IntechOpen

Author details

Dongmei Ye* and Susan Rempe
Sandia National Laboratories, Albuquerque, New Mexico, USA

*Address all correspondence to: dye@sandia.gov

IntechOpen

References

[1] Talabani JM, Ali AI, Kadir AM, Rashid R, Samin F, Greenwood D, et al. Long-term health effects of chemical warfare agents on children following a single heavy exposure. Human & Experimental Toxicology. 2018;**37**:836-847

[2] Smart JK, editor. History of Chemical and Biological Warfare: An American Perspective. Falls Church, Virginia: Office of The Surgeon General, Department of the Army; 2008. pp. 9-76

[3] Kim M, Gkikas M, Huang A, Kang JW, Suthiwangcharoen N, Nagarajan R, et al. Enhanced activity and stability of organophosphorus hydrolase via interaction with an amphiphilic polymer. Chemical Communication (Camb). 2014;**50**:5345-5348

[4] Otto TC, Harsch CK, Yeung DT, Magliery TJ, Cerasoli DM, Lenz DE. Dramatic differences in organophosphorus hydrolase activity between human and chimeric recombinant mammalian paraoxonase-1 enzymes. Biochemistry. 2009;**48**:10416-10422

[5] Benning MM, Shim H, Raushel FM, Holden HM. High resolution X-ray structures of different metal-substituted forms of phosphotriesterase from Pseudomonas diminuta. Biochemistry. 2001;**40**:2712-2722

[6] Wong KY, Gao J. The reaction mechanism of paraoxon hydrolysis by phosphotriesterase from combined QM/MM simulations. Biochemistry. 2007;**46**:13352-13369

[7] Koca J, Zhan CG, Rittenhouse RC, Ornstein RL. Mobility of the active site bound paraoxon and sarin in zinc-phosphotriesterase by molecular dynamics simulation and quantum chemical calculation. Journal of the American Chemical Society. 2001;**123**:817-826

[8] Gomes DE, Lins RD, Pascutti PG, Lei C, Soares TA. Conformational variability of organophosphorus hydrolase upon soman and paraoxon binding. The Journal of Physical Chemistry. B. 2011;**115**:15389-15398

[9] El Khoury L, Mobley DL, Ye D, Rempe SB. Enhancing Paraoxon binding to organophosphorus hydrolase active site. International Journal of Molecular Sciences. 2021;**22**:12624-12640

[10] Hopkins CW, Le Grand S, Walker RC, Roitberg AE. Long-time-step molecular dynamics through hydrogen mass repartitioning. Journal of Chemical Theory and Computation. 2015;**11**:1864-1874

[11] Darden TY, Pedersen L. Particle mesh Ewald: An N log (N) method for Ewald sums in large systems. The Journal of Chemical Physics. 1993;**98**:10089-10092

[12] Onufriev A, Bashford D, Case DA. Exploring protein native states and large-scale conformational changes with a modified generalized born model. Proteins. 2004;**55**:383-394

[13] Axelsen PHL. Improved convergence in dual-topology free energy calculations through use of harmonic restraints. Journal of Computational Chemistry. 1998;**19**:1278-1283

[14] Lewis VE, Donarski WJ, Wild JR, Raushel FM. Mechanism and stereochemical course at phosphorus of the reaction catalyzed by a bacterial phosphotriesterase. Biochemistry. 1988;**27**:1591-1597

[15] Aubert SD, Li Y, Raushel FM. Mechanism for the hydrolysis of organophosphates by the bacterial phosphotriesterase. Biochemistry. 2004;**43**:5707-5715

[16] Reeves TE, Wales ME, Grimsley JK, Li P, Cerasoli DM, Wild JR. Balancing the stability and the catalytic specificities of OP hydrolases with enhanced V-agent activities. Protein Engineering, Design & Selection. 2008;**21**:405-412

[17] Tinberg CE, Khare SD, Dou J, Doyle L, Nelson JW, Schena A, et al. Computational design of ligand-binding proteins with high affinity and selectivity. Nature. 2013;**501**:212-216

[18] Grisewood MJ, Gifford NP, Pantazes RJ, Li Y, Cirino PC, Janik MJ, et al. OptZyme: Computational enzyme redesign using transition state analogues. PLoS One. 2013;**8**:e75358

[19] Bjelic S, Kipnis Y, Wang L, Pianowski Z, Vorobiev S, Su M, et al. Exploration of alternate catalytic mechanisms and optimization strategies for retroaldolase design. Journal of Molecular Biology. 2014;**426**:256-271

[20] Rajagopalan S, Wang C, Yu K, Kuzin AP, Richter F, Lew S, et al. Design of activated serine-containing catalytic triads with atomic-level accuracy. Nature Chemical Biology. 2014;**10**:386-391

[21] Wild C, Cunningham KA, Zhou J. Allosteric modulation of G protein-coupled receptors: An emerging approach of drug discovery. Austin Journal of Pharmacological Therapy. 2014;**2014**:2

[22] De Smet F, Christopoulos A, Carmeliet P. Allosteric targeting of receptor tyrosine kinases. Nature Biotechnology. 2014;**32**:1113-1120

[23] Nickols HH, Conn PJ. Development of allosteric modulators of GPCRs for treatment of CNS disorders. Neurobiology of Disease. 2014;**61**:55-71

[24] Wang L, Martin B, Brenneman R, Luttrell LM, Maudsley S. Allosteric modulators of g protein-coupled receptors: Future therapeutics for complex physiological disorders. The Journal of Pharmacology and Experimental Therapeutics. 2009;**331**:340-348

[25] Karginov AV, Ding F, Kota P, Dokholyan NV, Hahn KM. Engineered allosteric activation of kinases in living cells. Nature Biotechnology. 2010;**28**:743-747

[26] Wenthur CJ, Gentry PR, Mathews TP, Lindsley CW. Drugs for allosteric sites on receptors. Annual Review of Pharmacology and Toxicology. 2014;**54**:165-184

[27] Wootten D, Christopoulos A, Sexton PM. Emerging paradigms in GPCR allostery: Implications for drug discovery. Nature Reviews. Drug Discovery. 2013;**12**:630-644

[28] Dokholyan NV. Controlling allosteric networks in proteins. Chemical Reviews. 2016;**116**:6463-6487

[29] Dagliyan O, Tarnawski M, Chu PH, Shirvanyants D, Schlichting I, Dokholyan NV, et al. Engineering extrinsic disorder to control protein activity in living cells. Science. 2016;**354**:1441-1444

[30] Dagliyan O, Shirvanyants D, Karginov AV, Ding F, Fee L, Chandrasekaran SN, et al. Rational design of a ligand-controlled protein conformational switch. Proceedings of the National Academy of Sciences of the United States of America. 2013;**110**:6800-6804

[31] Yin S, Ding F, Dokholyan NV. Modeling backbone flexibility improves protein stability estimation. Structure. 2007;**15**:1567-1576

[32] Yin S, Ding F, Dokholyan NV. Eris: An automated estimator of protein stability. Nature Methods. 2007;**4**:466-467

[33] Mee-Hie Cho C, Mulchandani A, Chen W. Functional analysis of organophosphorus hydrolase variants with high degradation activity towards organophosphate pesticides. Protein Engineering, Design & Selection. 2006;**19**:99-105